G3: Genes|Genomes|Genetics Early Online, published on March 31, 2015 as doi:10.1534/g3.115.017517

Analysis of RNA interference lines identifies new functions of maternally-expressed genes involved in embryonic patterning in *Drosophila melanogaster*

Niankun Liu and Paul Lasko*

Department of Biology, McGill University, 3649 Promenade Sir William Osler, Montréal, Québec, Canada H3G 0B1

*Corresponding author, tel +1 514 398 6721, fax +1 514 398 1684, e-mail paul.lasko@mcgill.ca

© The Author(s) 2013. Published by the Genetics Society of America.

Abstract

Embryonic patterning in *Drosophila melanogaster* is initially established through the activity of a number of maternally expressed genes that are expressed during oogenesis. mRNAs from some of these genes accumulate in the posterior pole plasm of the oocyte and early embryo, and localize further into RNA islands, transient ring-like structures that form around the nuclei of future primordial germ cells (pole cells) at stage 3 of embryogenesis. As mRNAs from several genes with known functions in anterior-posterior patterning and/or germ cell specification accumulate in RNA islands, we hypothesized that some other mRNAs that localize in this manner might also function in these developmental processes. To test this, we investigated the developmental functions of 51 genes whose mRNAs accumulate in RNA islands by abrogating their activity in the female germline using RNA interference. This analysis revealed requirements for *ttk*, *pbl*, *Hip14*, *eIF5*, *eIF4G*, and *CG9977* for progression through early oogenesis. We observed dorsal appendage defects in a proportion of eggs produced by females expressing double-stranded RNA targeting *Mkrn1* or *jvl*, implicating these two genes in dorsal-ventral patterning. In addition, posterior patterning defects and a reduction in pole cell number were seen in the progeny of *Mkrn1* females. As the mammalian orthologue of Mkrn1 acts as an E3 ubiquitin ligase, these results suggest an additional link between protein ubiquitination and pole plasm activity.

Introduction

mRNA localization to particular intracellular regions is widespread. In the early Drosophila embryo, mRNA localization, coupled to spatially-dependent translational regulation, contributes to targeting the proteins the localized mRNAs encode to the region of the embryo that is appropriate for their developmental function (Lécuyer et al. 2007; Kugler and Lasko 2009). Hundreds of mRNAs have been identified that accumulate in the posterior pole plasm of the early *Drosophila* embryo, where cytoplasmic determinants specify the germ line (Lécuyer et al. 2007, Fisher et al. 2012). While a great deal has been learned about how several of these mRNAs function in embryonic patterning and specifying the germ line, for the vast majority little is known about what role, if any, they have. Several maternal mRNAs that are essential for establishment of anterior-posterior pattern and for specification of germ cells, including *aret*, *exu*, *gcl*, *nos*, *orb*, *pgc*, and *spir*, are among approximately 50 known mRNAs that transiently accumulate in rings, sometimes termed 'RNA islands', that become apparent around the pole cell nuclei just prior to completion of their cellularization (Lécuyer et al. 2007, images publicly available at http://fly-fish.ccbr.utoronto.ca). This suggests a fundamental role for these perinuclear structures, and their constituent mRNAs, in embryonic patterning and germ cell specification. However, the functions of most mRNAs that localize to these structures in pattern formation or germ cell specification are unknown, because mutations affecting them are lethal, or because mutations block oogenesis before mature eggs that can be fertilized are formed, or because no mutants are available.

To address germline-specific functions of essential genes, genetic approaches have been developed to abrogate the functions of specific genes only in germline cells. One such approach involves inducing mitotic recombination and selecting for recombinants using a chromosome carrying a dominant female sterile mutation (Perrimon and Gans 1983). This technique has been used to screen for maternal functions of many zygotically essential genes (Perrimon et al. 1984; Perrimon et al. 1989); however it is laborious and such screens have yet to be extended to the entire genome. A more recent approach to this problem is based upon the principle of RNA interference (RNAi), in which expression of a small double-stranded hairpin RNA (shRNA) including sequences homologous to a target mRNA post-transcriptionally inactivates the target through translational repression and degradation (Fire et al. 1998). Publicly accessible libraries of Drosophila lines that express shRNA targeting most protein-coding genes under the control of the upstream activation sequence (UAS) have been assembled (Mummery-Widmer et al. 2009; Ni et al. 2011). With the use of the appropriate GAL4 driver, these enable in principle the specific inactivation of nearly any gene in any tissue, including germline.

To investigate potential functions of mRNAs that accumulate in RNA islands in embryonic patterning or germ cell specification, in this work we conducted a comprehensive analysis of the phenotypes that result during oogenesis or in progeny embryos from maternal germline specific expression of shRNA that targets each mRNA that accumulates in these perinuclear structures.

Materials and Methods

Drosophila strains

shRNA-expressing stocks were obtained from the Bloomington stock center, and the stock numbers are shown in Table 1. The full genotypes of all the lines used in this study are available on the TRiP website (http://www.flyrnai.org/TRiP-HOME.html). We used the maternal triple driver *MTD-Gal4* to induce expression of shRNA in germ line cells throughout oogenesis (Petrella *et al*. 2007), and obtained this stock as well from the Bloomington stock center (stock number 31777).

Screen setup

10-15 *MTD-Gal4* males were crossed to 10-15 virgin females of each TRiP line in a vial, and transferred to fresh food every 3-5 days. Crosses were incubated either at 25° C throughout the experiment, or alternatively the flies were discarded after five days and the vials containing larvae were transferred to 29° C to complete development. Growth of females with MTD-Gal4 driven shRNAs at 29° C sometimes produces more severe phenotypes and more effective knockdown of the target mRNA (Ni et al. 2011, this study). Progeny carrying both *MTD-Gal4* and the shRNA construct were collected from these crosses, eggs were collected, and their phenotypes were assessed as described below.

Cuticle preparation, hatch rate determination and dorsal appendage preparation

Cuticle preparations were done as described in (Nüsslein-Volhard *et al*. 1984) with the following modifications. 30-50 flies, of both sexes in approximately equal proportions, were transferred into egg-laying cages with apple juice agar plates (60 mm x 15 mm cell culture dish) supplemented with fresh yeast paste and incubated at 25° C or 29° C. Genotypes for these crosses are described in Results. Collections from the first two days after transfer were discarded. Subsequently, eggs were collected either overnight or for 6 hr, and allowed to develop for an additional 36 hr at 25° C. Hatch rate was determined by counting the number of hatched eggs and unhatched eggs for each lay. In cases where more than 20% of the eggs failed to hatch, eggs were collected for cuticle preparation as follows. Embryos were transferred into small sieves and washed with water first, then dechorionated in a 50% dilution of commercial bleach (12% sodium hypochlorite) for 2 min, and washed with water for another 2 min. The embryos were then transferred with a fine brush into a 1.5 ml microcentrifuge tube containing PBST buffer (1 X PBS, and 0.1% Tween-20). Buffer was removed as completely as possible with a micropipette tip, and 30 µl Hoyer's medium (30 g gum arabic, 50 ml H_2O, 200 g chloral hydrate, 20 g glycerol) was added. The embryos were then mounted onto a glass slide and covered with a 22 X 22 mm cover slip. Next, the embryos were cleared by overnight incubation at 65° C, and observed under dark field illumination using a Leica DM 6000B microscope. To assess dorsal appendage phenotypes, newly laid eggs were transferred onto a

glass slide containing PBST buffer, and examined under dark field illumination using a Leica DM 6000B microscope.

Immunohistochemistry

Ovaries were dissected from 3- to 5-day-old females in PBS and fixed in 100 µl of PBS, 1% NP-40, 600 µl of heptane, and 100 µl of 10% formaldehyde for 20 min. Samples were rinsed three times, washed three times for 10 min with PBST (PBS + 0.3% Triton X-100), and blocked in PBSTA (PBST + 1% BSA) for 1 h at room temperature. Samples were incubated with primary antibodies overnight at 4° C in PBSTA. Samples were rinsed three times, washed three times (20 min each) with PBST, then blocked in 1 ml of PBSTA for 1 h at room temperature. Samples were incubated in the dark with fluorescent secondary antibody (pre-adsorbed goat anti-rat Alexa Fluor 488 and goat anti-rabbit Alexa Fluor 555, Life Technologies), final dilution 1:1000 in PBSTA overnight at 4° C, then washed four times (5 min each) and twice (15 min each) in PBST in the dark. Samples were counterstained with DAPI, mounted in anti-fade reagent in glycerol/PBS from the SlowFade Antifade Kit (Molecular Probes), and examined under a confocal microscope (Zeiss LSM510). Rat anti-Vas was used at a dilution of 1:1000. Rabbit anti-Osk was used at a dilution of 1:1000. Embryos were immunostained as described in (Kobayashi *et al.* 1999). Primary rabbit anti-Vas was used at 1:5000. Secondary antibody was anti-rabbit Alexa Fluor 488 (Life technologies). Images were collected on a Leica DM 6000 B microscope.

RNA isolation and RT-PCR analysis

Total RNA was prepared from 30 embryos (0-2 hr at 25° C or 0-1 hr at 29° C) using TRIzol® reagent (Life Technologies) according to the manufacturer's protocol, followed by treatment with TURBO DNase (Ambion) for 30 min at 37°C. First strand cDNA was synthesized with Maxima H Minus First Strand cDNA Synthesis Kit (Thermo Scientific). Quantitative differences in gene expression were determined by PCR with JumpStart REDTaq ReadyMix Reaction Mix (Sigma) using the first strand cDNA as a template. PCR products (5 µL for each) were resolved on a 1.5% agarose gel, using primers that produced a product between 150-250 bp in length. Primers that amplify *rp49* mRNA served as a positive control.

Results

Our results are described below and also summarized in tabular form (Table 1).

Maternal-effect loci involved in embryonic patterning

We examined cuticle preparations from embryos produced by females expressing each RNA interference construct (henceforth referred to as knockdown embryos for brevity) that failed to hatch into larvae as a first step in characterizing their phenotype. In wild-type embryos that are about to hatch, the most prominent anterior structures are the mouth parts, which protrude from the anterior pole into the interior of the embryo (Fig. 1, **wt**, seen most easily in the leftmost panel). Three thoracic segments and eight abdominal segments are then marked by transverse bands of short bristles called denticle belts; these are very fine and narrow for the

three thoracic segments, but broader and more prominent for the eight abdominal segments (Fig. 1, **wt**). At the most posterior structure is a pair of structures, collectively termed the telson (Fig. 1, **wt**, seen most easily in the rightmost panel).

Consistent with known phenotypes for the corresponding mutants (Lehmann and Nüsslein-Volhard 1986, Schüpbach and Wieschaus 1986, Nüsslein-Volhard et al. 1987; Manseau and Schüpbach 1989), most o*sk*, *nos, spir* and *vas* knockdown embryos exhibited a strong grandchildless-*knirps* phenotype (Schüpbach and Wieschaus 1986). These embryos are shorter than wild-type, lack most posterior segmentation, and have two prominent foci of telson-derived material, surrounded by mostly naked cuticle (Fig. 1; ***osk, nos, spir, vas***). A substantial proportion (~25%) of *nos* embryos cultured at 29°C completely failed to develop and did not form cuticle. Interestingly, we discovered a similar grandchildless-*knirps* phenotype in 5-10% of *mkrn1* knockdown embryos that failed to hatch (Fig. 1, ***mkrn1****,* left and center panels), although posterior defects were less extreme in some of these embryos with most posterior denticle belts apparent (Fig. 1, ***mkrn1***, right panel). Severe posterior patterning defects were also observed in some *Rapgap1*, *CAH2*, *Patr-1*, and *jvl* embryos (Fig. 1, ***Rapgap1, CAH2, Patr-1, jvl***). These embryos differed from grandchildless-*knirps* embryos, however, in that most did not completely fill the entire volume of the egg and appeared shrivelled, presumably as a result of holes in their cuticles. For *CAH2* and *Patr-1* these phenotypes were incompletely penetrant and many embryos appeared normal, while for *Rapgap1* and *jvl* most embryos were affected. *CG31998* knockdown embryos also exhibited defects in anterior-posterior patterning, but to a

lesser degree than for those previously mentioned. In some *CG31998* knockdown embryos, the fourth abdominal segment was partially or fully absent, or fused with the fifth (Fig. 1, ***CG31998***).

Consistent with the known phenotype for the corresponding mutant (Schüpbach and Wieschaus 1989), *cta* knockdown embryos failed to properly complete gastrulation. The embryos form a twisted structure with anterior holes (Fig. 1, ***cta***). *Tao* knockdown embryos progress through germ band extension but then do not retract, so they form U-shaped cuticles (Fig. 1, ***Tao***). These embryos also have obvious head defects. In *milt* knockdown embryos various segments are partially missing or are fused, telsons are also often missing or reduced to rudiments (Fig. 1, ***milt***). *del*, *gwl*, *CG4040, nrv1* and *exu* knockdown embryos do not progress sufficiently in development to form cuticles (Fig. 1, ***del, gwl, CG4040, nrv1, exu***); however, for *exu* and *gwl* (Fig. 2) this phenotype is somewhat suppressed by a wild-type paternal copy of the gene, in that cuticles form but severe anterior-posterior patterning defects are apparent including a loss of anterior structures (Fig. 1, ***exu with wt male***). Loss of anterior structures has been reported as a maternal-effect phenotype of *exu* mutations (Schüpbach and Wieschaus 1989), and failure of oocytes to arrest in metaphase I of meiosis, resulting in a failure to support embryogenesis, is a phenotype of a hypomorphic *gwl* allele (Archambault et al. 2007). Finally, in many *CG9821* knockdown embryos mouth parts are malformed and there is loss or fusion of abdominal segments (Fig. 1, ***CG9821***). Other *CG9821* knockdown embryos are however patterned normally.

Examination of pole cells in knockdown embryos with defects in embryonic development, and assessment of dorsal appendages

Next, we examined these knockdown embryos for their ability to form pole cells by immunostaining with anti-Vas (Fig. 2). In wild-type, pole cells form at the posterior pole prior to general cellularization (Fig. 2A, left panel). At gastrulation they migrate along with the posterior midgut invagination into the interior of the embryo, then migrate as individual cells (Fig. 2A, right panel), until forming two clusters in association with the gonadal mesoderm to form the two gonads. Knockdown embryos for known posterior-group genes (*vas, osk, spir*; Fig. 2B, 2E, 2H), and those that did not form cuticle (*del, gwl, exu, nrv1, CG4040*; Fig. 2I, 2J, 2L, 2N, 2P) also did not form pole cells, although this phenotype was completely rescued for *exu* (Fig. 2M), and partially rescued for *gwl* (Fig. 2K), by a paternal wild-type copy of the gene . In this case approximately 50% of *gwl* knockdown embryos formed pole cells in numbers smaller than wild-type. Consistent with the phenotype of the corresponding mutant, and that of embryos produced by females expressing antisense RNA targeting *pgc* (Nakamura et al. 1996, Martinho et al. 2004), we observed a severe reduction in pole cell number in *pgc* knockdown embryos; pole cells were absent in 20% of embryos and present in reduced numbers in the remaining 80% (Fig. 2F). For *CG31998*, 15% of knockdown embryos formed 0-5 pole cells and the rest formed wild-type numbers of pole cells (Fig. 2C). A similar phenotype was observed for *Mkrn1*, with approximately 20% of embryos forming 0-5 pole cells (Fig. 2D). Pole cells were also absent in approximately 25% of *Rapgap1* embryos (Fig. 2G). For *nos* knockdown embryos cultured at 29°C, pole cells formed in normal numbers and were localized normally until the onset of pole cell migration (Fig. 2O, left panel). In later-stage embryos pole cell migration was highly

aberrant and pole cell numbers diminished as development progressed, such that stage 14 and later embryos had only a few scattered pole cells (Fig. 2O, right panel), or none at all. In knockdown embryos for *Tao*, *milt*, and *cta*, wild-type numbers of pole cells form, but they also frequently scattered during migration. This is presumably because of the extensive somatic defects that are present in these embryos. We observed failure of pole cells to coalesce into gonads in 53% of *Tao* knockdown embryos, 36% of *milt* knockdown embryos, and 97% of *cta* knockdown embryos (Fig. 3). Our results differ from observations of embryos produced by a *Tao* hypomorphic mutant where reduced numbers of pole cells were present (Sato et al. 2007). We also observed defects in dorsal appendage structure in eggs produced by *Mkrn1* and *jvl* knockdown females (Fig. 4). For *Mkrn1* knockdowns, 15% of eggs lacked dorsal appendages while 18% had a single fused dorsal appendage, while for *jvl* knockdowns, 19% of eggs lacked dorsal appendages while 24% had a single fused dorsal appendage. Similar dorsal appendage defects have been reported in eggs produced from a hypomorphic *jvl* mutant (Dubin-Bar et al. 2011).

Knockdown of some genes blocked oogenesis

Knockdown of another set of genes whose mRNAs accumulate in pole cell rings resulted in defects during oogenesis that prevented the development of mature eggs. In these cases we analyzed the morphology of the ovaries that were produced (Fig. 5). The earliest developmental blocks in oogenesis occurred in females knocked down for *pbl* (Fig. 5C), *Hip14* (Fig. 5E), *eIF5* (Fig. 5F), or *CG9977* (Fig. 5I). In these cases essentially no germ line cells were observed, indicating that abrogation of function of these genes results in cellular lethality.

Knockdown of *orb* (Fig. 5D), *eIF-4G* (Fig. 5G), or *aret* (Fig. 5H) resulted in the formation of some rudimentary egg chambers, but these did not progress beyond early pre-vitellogenic stages. The phenotypes of *orb* and *aret* knockdowns are consistent with those of known severe mutations in these genes (Schüpbach and Wieschaus 1991, Christerson and McKearin 1994). Knockdown of *mei-P26* led to the formation of tumorous egg chambers similar to those described in *mei-P26* mutants (Fig. 5J) (Page et al. 2000). Knockdown of *ttk* resulted in normal oogenesis until approximately stage 6, followed by extensive cell death (Fig. 5B).

Assessment of efficacy of RNAi knockdown

We examined the effectiveness of each RNAi construct at targeting its corresponding mRNA using RT-PCR (Fig. 6). In total we attempted to knock down the germline activities of 51 different genes that express mRNAs that localize in perinuclear rings in the precursors to pole cells. For seven of these genes [*Bsg25D* (Fig. 6F7), *CG18446* (Fig. 6B7) *charybde* (Fig. 6F6), *cta* (Fig. 6E7), *pAbp* (Fig. 6B9), *pgc* (Fig. 6F9), *Pino* (Fig. 6E8)], the effectiveness of the knockdowns appeared very poor (<40% reduction) by this assay, even when flies were cultured at elevated temperature. While we did not observe any effects on oogenesis or embryonic viability from expressing shRNA targeting *Bsg25D, CG18446, charybde, pAbp*, or *Pino*, we cannot conclude that these genes play no essential role in the female germ line because targeting them in this way was inefficient. Surprisingly, despite apparently poor efficiency of the corresponding shRNA we nevertheless obtained a developmental phenotype for *cta* and *pgc*, as described in earlier sections. For *ttk*, knockdown was poor when shRNA expressing flies were cultured at

25°C (Fig. 6F4) and no phenotype resulted, but culture at 29°C resulted in an early block in oogenesis (Fig. 5), presumably implying effective knockdown but also making it impossible to collect embryos for RT-PCR analysis.

Conversely, knockdown of 27 genes appeared complete or nearly so (80-100%) by RT-PCR at one or both temperature conditions. These genes in alphabetical order were *Ack* (Fig. 6C2), *CAH2* (Fig. 6G6), *CG4040* (Fig. 6G1), *CG5292* (Fig. 6A7), *CG6509* (Fig. 6A10), *CG10077* (Fig. 6A6), *CG31998* (Fig. 6A8), *CycB* (Fig. 6C8), *del* (Fig. 6A5), *dock* (Fig. 6D8), *exu* (Fig. 6A2), *Gap1* (Fig. 6F1), *gcl* (Fig. 6D10), *gwl* (Fig. 6A4), *jvl* (Fig. 6E9), *milt* (Fig. 6A1), *Mkrn1* (Fig. 6E6), *nrv1* (Fig. 6F5), *osk* (Fig. 6D1), *Patr-1* (Fig. 6B8), *PI3K21B* (Fig. 6B10), *pum* (Fig. 6C9), *Rapgap1* (Fig. 6D9), *Tao* (Fig. 6A3), *Tm1* (Fig. 6D3), *Unr* (Fig. 6B6), and *vas* (Fig. 6H2). The phenotypes of *MTD-Gal4* driven expression of shRNAs targeting 15 of these genes (*CAH2, CG4040, CG31998, del, exu, gwl, jvl, milt, Mkrn1, nrv1, osk, Patr-1, Rapgap1, Tao,* and *vas*) have been described above. For the other 12 (*Ack, CG5292, CG6509, CG10077, CycB, dock, Gap1, gcl, PI3K21B, pum, Tm1*, and *Unr*) we observed no effect on oogenesis or embryonic development. This is a surprising result for *gcl* and *pum* as the requirements for *gcl* in germ line for establishment of the germ cell lineage and of *pum* for posterior patterning and germ cell maintenance are well established (Asaoka-Taguchi et al. 1999; Parisi and Lin 1999; Robertson et al. 1999). We also expected to observe phenotypes in *Tm1* knockdown embryos because several *Tm1* mutations virtually abrogate *osk* localization and germline clones of a *Tm1* null allele produce sterile adults or embryos lacking germ cells and abdominal segments (Erdélyi et al. 1995). As well, *CycB* mutants are female sterile and produce rudimentary ovaries (Jacobs et al. 1998). We conclude that even in cases

where knockdown appears efficient, lack of a phenotype from shRNA expression does not rule out involvement of a particular gene in oogenesis or embryonic patterning.

Our attempts at knockdown of eight other genes were only partially successful (40-80%). These genes in alphabetical order were *Ank* (Fig. 6E10), *CG2865* (Fig. 6C10), *CG9821* (Fig. 6D6), *CG11597* (Fig. 6D7), *nos* (Fig. 6F10), *sl* (Fig. 6A9), *spir* (Fig. 6F8), and *sra* (Fig. 6C6). As discussed above, we nevertheless obtained phenotypes from knockdown of *CG9821*, *nos*, and *spir*, but it remains possible that more severe phenotypes, or phenotypes that manifest earlier, would have been observed if the knockdowns were more efficient. For the remainder of these genes where partial knockdowns did not produce effects on oogenesis or embryogenesis, we cannot draw any conclusions about potential roles for them in these processes.

For the nine genes, including *ttk* at 29 °C, for which knockdown produced developmental blocks in early stages in oogenesis (Fig. 5), we did not analyze the effectiveness of the knockdown in this manner, because tissue from their rudimentary ovaries was difficult to obtain and appropriate controls were lacking.

Finally, we examined whether two pole plasm components, Osk and Vas protein, localized normally to the posterior of the stage-10 oocyte in the knockdown lines where pole cell formation was compromised. In flies expressing shRNA targeting *del*, we found that posterior accumulation of both Osk and Vas was greatly reduced, as was accumulation of Vas into the perinuclear nuage, but that the level of Vas in the cytoplasm of nurse cells was comparable to

controls (Fig. 7). Conversely, for flies expressing shRNA targeting *CG4040, exu, gwl*, or *nrv1*, Vas and Osk accumulation appeared similar to wild-type (data not shown).

Discussion

In this study we analyzed a set of mRNAs, that accumulate in cytoplasmic rings within primordial germ cell precursors, sometimes called 'RNA islands', by expressing in germ line shRNAs that target them, and examining the phenotypic consequences. This work provided evidence for specific roles in embryonic patterning and/or germ line specification for several genes whose mRNAs localize in this way and that have not previously been implicated in these processes. This provides further support for the conclusion that these structures accumulate mRNAs that are involved in these developmental events.

Of particular interest to us are genes that we implicated in anterior-posterior embryonic patterning or in germ cell specification. One of these is *mkrn1*, for which no mutant phenotype had previously been described in *Drosophila*. In mammals, the protein encoded by MKRN1 is an E3 ubiquitin ligase that modifies PPARγ, a transcription factor involved in activating adipocyte differentiation, and targets it for degradation (Kim et al. 2014). Several other targets have also been identified for MKRN1, indicating it is involved in numerous cellular and disease-related processes. Previous work has implicated post-translational modification pathways in establishing and maintaining posterior localization of Vas (Liu et al. 2003; Kugler et al. 2010), and thus in anterior-posterior patterning and pole cell specification. Our present observations

raise the possibility that Mkrn1 may regulate the stability by ubiquitinating one or more proteins involved in posterior patterning and pole cell specification.

We also observed posterior embryonic defects in *Patr-1* knockdown embryos. *Patr-1* encodes a component of P bodies that is believed to activate mRNA decapping and miRNA degradation (Jäger and Dorner 2010, Pradhan et al. 2012, Barišić-Jäger et al. 2013, Nishihara et al. 2013), and it has also been identified as a component of the somatic piRNA pathway (Handler et al. 2013). It has been demonstrated that Patr-1 interacts with the CCR4 deadenylase at the larval neuromuscular junction (Pradhan et al. 2012), but its role in germline development has heretofore been unexplored. Given the well-established importance of decapping and CCR4-mediated deadenylation in post-transcriptional genetic regulation in the female germline (Zaessinger et al. 2006, Chicoine et al. 2007, Tadros et al. 2007, Rouget et al. 2010, Igreja and Izaurralde 2011), it is probable that the phenotype we observed in *Patr-1* knockdown embryos results from effects on these processes.

The other RNA knockdown lines that produced maternal-effect anterior-posterior defects were *jvl*, *Rapgap1*, and *CAH2*. *jvl* encodes a microtubule-associated protein, and *jvl* mutant oocytes show defects in localization of *grk*, *bcd*, and *osk* mRNA as well as disruptions of the cytoskeleton (Dubin-Bar et al. 2011). Both the mutant and our knockdown line produced embryos with dorsal appendage defects, confirming a role for *jvl* in the germline in producing these structures. Dorsal appendages are produced by follicle cells in response to activation of the epidermal growth factor receptor (Egfr) by its ligand Grk, which is translated in the oocyte

from the localized *grk* mRNA and secreted over a short range (González-Reyes et al. 1995; Roth et al. 1995). While we did not analyze *grk* mRNA localization in *jvl* (or *Mkrn1*) knockdown embryos because their dorsal appendage phenotypes were not fully penetrant, effects on *grk* mRNA localization, as observed in the *jvl* mutant (Dubin-Bar et al. 2011), could explain the effects we observed in these knockdown embryos on dorsal appendage formation.

Unlike in the corresponding mutant, in *jvl* knockdown embryos we did not observe defects in posterior Osk or Vas localization, possibly because of incomplete inactivation of the *jvl* mRNA. Conversely, while the defect in *osk* localization in the *jvl* mutant would be expected to lead to anterior-posterior defects in progeny embryos, this was not observed, because *jvl* mutant eggs do not support embryogenesis beyond initial stages. In this instance then the incomplete knockdown (or germline specificity of the knockdown) of the target mRNA allowed the identification of a phenotype that was masked in a strong mutant allele. Another similar instance concerned *del*; *del* mutant alleles block oogenesis at an early stage (Schüpbach and Wieschaus 1991), and Del protein has recently been identified as a component of a complex that is targeted to chromatin at dual-strand piRNA clusters and required to produce piRNAs from those clusters (Mohn et al. 2014). While analysis of rare escaper eggs that progress more completely through oogenesis indicated a later role for *del* in microtubule-mediated processes including localization of *osk* and *grk* mRNAs (Wehr et al. 2006), this later phenotype is much more apparent in the RNA knockdown line that produces substantial numbers of embryos.

It is more difficult to predict potential functions for the other two genes in embryonic patterning or germ line specification. *Rapgap1* encodes a GTPase activator involved in intracellular signalling, but a null mutant for this gene has been reported to be viable and fertile, with only minor irregularities in pole cell alignment at embryonic stage 13 (Chen et al. 1997). Further work will be necessary to determine whether the phenotype we observed results from a secondary off-target effect of the *Rapgap1* shRNA. *CAH2* is one of two *Drosophila* genes that encodes a carbonic anhydrase, an enzyme that catalyzes the reversible hydration of carbon dioxide to bicarbonate (Syrjänen et al. 2013). No mutant phenotype has been reported for this gene. It is likely to be functionally redundant with CAH1 in most tissues, but high-throughput data indicates that CAH2 is by far the predominant form of the enzyme that is expressed in ovaries (Graveley et al. 2011). A role for glycolytic enzymes in germ cell development has recently been described, indicating that metabolic enzymes can have specific developmental roles (Gao et al. 2015).

Acknowledgments

We are grateful to Sanjay Ghosh for much helpful advice about using the Trip lines. This work was supported by grant IOP-107945 from the Canadian Institutes of Health to P. L.

References

Archambault, V., X. Zhao, H. White-Cooper, A. T. Carpenter, and D. M. Glover, 2007 Mutations in *Drosophila* Greatwall/Scant reveal its roles in mitosis and meiosis and interdependence with Polo kinase. PLoS Genet. 3(11): e200.

Asaoka-Taguchi, M., M. Yamada, A. Nakamura, K. Hanyu, and S. Kobayashi, 1999 Maternal Pumilio acts together with Nanos in germline development in Drosophila embryos. Nat. Cell Biol. 1: 431-437.

Barišić-Jäger, E., I. Kręcioch, S. Hosiner, S. Antic, and S. Dorner, 2013 HPat a decapping activator interacting with the miRNA effector complex. PLoS ONE 8(8):e71680.

Chen, F., M. Barkett, K. T. Ram, A. Quintanilla, and I. K. Hariharan, 1997 Biological characterization of *Drosophila* Rapgap1, a GTPase activating protein for Rap1. Proc. Natl. Acad. Sci. USA 94: 12485-12490.

Chicoine, J., P. Benoit, C. Gamberi, M. Paliouras, M. Simonelig, and P. Lasko, 2007 Bicaudal-C recruits CCR4-NOT deadenylase to target mRNAs and regulates oogenesis, cytoskeletal organization, and its own expression. Dev. Cell 13: 691-704.

Christerson, L. B. and D. McKearin, 1994 *orb* is required for anteroposterior and dorsoventral patterning during *Drosophila* oogenesis. Genes Dev. 8: 614-628.

Dubin-Bar, D., A. Bitan, A. Bakhrat, S. Amsalem, and U. Abdu, 2011 *Drosophila javelin-like* encodes a novel microtubule-associated protein and is required for mRNA localization during oogenesis. Development 138: 4661-4671.

Erdélyi, M., A.-M. Michon, A. Guichet, J. B. Glotzer, and A. Ephrussi, 1995 Requirement for Drosophila cytoplasmic tropomyosin in *oskar* mRNA localization. Nature 377: 524-527.

Fire, A., S. Xu, M. K. Montgomery, S. A. Kostas, S. E. Driver, and C. C. Mello, 1998 Potent and specific genetic interference by double-stranded RNA in *Caenorhaebditis elegans*. Nature 391: 806-811.

Fisher, B., R. Weiszmann, E. Frise, A. Hammonds, P. Tomancak, et al., 2012 BDGP insitu homepage http://insitu.fruitfly.org/cgi-bin/ex/insitu.pl

Gao, M., T. C. Thomson, T. M. Creed, S. Tu, S. N. Loganathan, et al., 2015 Glycolytic enzymes localize to ribonucleoprotein granules in *Drosophila* germ cells, bind Tudor and protect them from transposable elements. EMBO Rep. 16: 379-386.

González-Reyes, A., H. Elliott, and D. St Johnston, 1995 Polarization of both major body axes in *Drosophila* by *gurken-torpedo* signalling. Nature 375: 654-658.

Graveley, B. R., A. N. Brooks, J. W. Carlson, M. O. Duff, J. M. Landolin, et al. 2011 The developmental transcriptome of *Drosophila melanogaster*. Nature 471: 473-479.

Handler, D., K. Meixner, M. Pizka, K. Lauss, C. Schmied, et al., 2013 The genetic makeup of the *Drosophila* piRNA pathway. Mol. Cell 50: 762-777.

Igreja, C. and E. Izaurralde, 2011 CUP promotes deadenylation and inhibits decapping of mRNA targets. Genes Dev. 25: 1955-1967.

Jacobs, H. W., J. A. Knoblich, and C. F. Lehner, 1998 *Drosophila* Cyclin B3 is required for female fertility and is dispensable for mitosis like Cyclin B. Genes Dev. 12: 3741-3751.

Jäger, E. and S. Dorner, 2010 The decapping activator HPat is a novel factor co-purifying with GW182 from *Drosophila* cells. RNA Biol. 7: 381-385.

Kim, J.-H., K. W. Park, E.-W. Lee, W.-S. Jang, J. Seo, et al., 2014 Suppression of PPARγ through MKRN1-mediated ubiquitination and degradation prevents adipocyte differentiation. Cell Death Diff. 21: 594-603.

Kobayashi, S., R. Amikura, A. Nakamura, and P. F. Lasko, 1999 Techniques for analyzing protein and RNA distribution in *Drosophila* ovaries and embryos at structural and ultrastructural resolution, pp. 426-445 in *Advances in molecular biology: a comparative methods approach to the study of oocytes and embryos*, edited by J. Richter, Oxford University Press, Oxford, UK.

Kugler, J.-M. and P. Lasko, 2009 Localization, anchoring and translational control of *oskar, gurken, bicoid*, and *nanos* mRNA during *Drosophila* oogenesis. Fly 3: 15-28.

Kugler, J.-M, J. S. Woo, B.H. Oh, and P. Lasko, 2010 Regulation of *Drosophila* Vasa in vivo through paralogous cullin-RING E3 ligase specificity receptors. Mol. Cell. Biol. 30: 1769-1782.

Lécuyer, E., H. Yoshida, N. Parthasarathy, C. Alm, T. Babak, et al., 2007 Global analysis of mRNA localization reveals a prominent role in organizing cellular architecture and function. Cell 131: 174-187.

Lehmann, R. and C. Nüsslein-Volhard, 1986 Abdominal segmentation, pole cell formation and embryonic polarity require the localized activity of *oskar*, a maternal gene in *Drosophila*. Cell 47: 141-152.

Liu, N., D. A. Dansereau, and P. Lasko, 2003 Fat facets interacts with Vasa in the *Drosophila* pole plasm and protects it from degradation. Curr. Biol. 13: 1905-1909.

Manseau, L. and T. Schüpbach, 1989 *cappuccino* and *spire*: two unique maternal-effect loci requires for both the anteroposterior and dorsoventral patterns of the *Drosophila* embryo. Genes Dev. 3: 1437-1452.

Martinho, R. G., P. S. Kunwar, J. Casanova, and R. Lehmann, 2004 A noncoding RNA is required for the repression of RNApolII-dependent transcription in primordial germ cells. Curr. Biol. 14: 159-165.

Mohn, F., G. Sienski, D. Handler, and J. Brennecke, 2014 The Rhino-Deadlock-Cutoff complex licenses noncanonical transcription of dual-strand piRNA clusters in *Drosophila*. Cell 157: 1364-1379.

Mummery-Widmer, J. L., M. Yamazaki, T. Stoeger, M. Novatchkova, S. Bhalerao, et al., 2009 Genome-wide analysis of Notch signalling in *Drosophila melanogaster*. Nature 458: 987-992.

Nakamura, A., R. Amikura, M. Mukai, S. Kobayashi, and P. F. Lasko, 1996 Requirement for a noncoding RNA in *Drosophila* polar granules for germ cell establishment. Science 274: 2075-2079.

Ni, J.-Q., R. Zhou,. B. Czech, L.-P. Liu, L. Holderbaum, et al., 2011 A genome-scale shRNA resource for transgenic RNAi in *Drosophila*. Nat. Methods 8: 405-407.

Nishihara, T., L. Zekri, J. E. Braun, and E. Izaurralde, 2013 miRISC recruits decapping factors to miRNA targets to enhance their degradation. Nucl. Acids Res. 41: 8692-8705.

Nüsslein-Volhard, C., E. Wieschaus, and H. Kluding, 1984 Mutations affecting the pattern of the larval cuticle in *Drosophila melanogaster*. Roux's Arch. Dev. Biol. 193: 267-282.

Nüsslein-Volhard, C., H.-G. Frohnhöfer, and R. Lehmann, 1987 Determination of anteroposterior polarity in *Drosophila*. Science 238: 1675-1681.

Page, S. L., K. S. McKim, B. Deneen, T. L. van Hook, and R. S. Hawley, 2000 Genetic studies of *mei-P26* reveal a link between the processes that control germ cell proliferation in both sexes and those that control meiotic exchange in *Drosophila*. Genetics 155: 1757-1772.

Parisi, M. and H. Lin, 1999 The *Drosophila pumilio* gene encodes two functional protein isoforms that play multiple roles in germline development, gonadogenesis, oogenesis and embryogenesis. Genetics 153: 235-250.

Perrimon, N. and M. Gans, 1983 Clonal analysis of the tissue specificity of recessive female sterile mutations of *Drosophila melanogaster* using a dominant female sterile mutation *Fs(1)K1237*. Dev. Biol. 100: 365-373.

Perrimon, N, L. Engstrom, and A. P. Mahowald, 1984 The effects of zygotic lethal mutations on female germ-line functions in *Drosophila*. Dev. Biol. 105: 404-414.

Perrimon, N., L. Engstrom, and A. P. Mahowald, 1989 Zygotic lethals with specific maternal effect phenotypes in *Drosophila melanogaster*. I. Loci on the X chromosome. Genetics 121: 333-352.

Petrella, L. N., T. Smith-Leiker, and L. Cooley, 2007 The Ovhts polyprotein is cleaved to produce fusome and ring canal proteins required for *Drosophila* oogenesis. Development 134: 703–712.

Pradhan, S. J., K. R. Nesler, S. F. Rosen, Y. Kato, A. Nakamura, et al., 2012 The conserved P body component HPat/Pat1 negatively regulates synaptic terminal growth at the larval *Drosophila* neuromuscular junction. J. Cell Sci. 125: 6105-6116.

Robertson, S. E., T. C. Dockendorff, J. L. Leatherman, D. L. Faulkner, and T. A. Jongens, 1999 *germ cell-less* is required only during the establishment of the germ cell lineage of *Drosophila* and has activities which are dependent and independent of its localization to the nuclear envelope. Dev. Biol. 215: 288-297.

Roth, S., F. S. Neuman-Silberberg, G. Barcelo, and T. Schüpbach, 1995 *cornichon* and the EGF receptor signalling process are necessary for both anterior-posterior and dorsal-ventral pattern formation in *Drosophila*. Cell 81: 967-978.

Rouget, C., C. Papin, A. Boureux, A. C. Meunier, B. Franco, et al., 2010 Maternal mRNA deadenylation and decay by the piRNA pathway in the early *Drosophila* embryo. Nature 467: 1128-1132.

Sato, K., Y. Hayashi, Y. Ninomiya, S. Shigenobu, K. Arita, et al., 2007 Maternal Nanos represses *hid/skl*-dependent apoptosis to maintain the germ line in *Drosophila* embryos. Proc. Natl. Acad. Sci. USA 104: 7455-7460.

Schüpbach, T. and E. Wieschaus, 1986 Maternal-effect mutations altering the anterior-posterior pattern of the *Drosophila* embryo. Roux's Arch. Dev. Biol. 195: 302-317.

Schüpbach, T. and E. Wieschaus, 1989 Female sterile mutations on the second chromosome of *Drosophila melanogaster*. I. Maternal effect mutations. Genetics 121: 101-117.

Schüpbach, T. and E. Wieschaus, 1991 Female sterile mutations on the second chromosome of *Drosophila melanogaster*. II. Mutations blocking oogenesis or altering egg morphology. Genetics 129: 1119-1136.

Syrjänen, L., M. E. Tolvanen, M. Hilvo, D. Vullo, F. Carta, et al., 2013 Characterization, bioinformatic analysis and dithiocarbamate inhibition studies of two new α-carbonic

anhydrases, CAH1 and CAH2, from the fruit fly *Drosophila melanogaster*. Bioorg. Med. Chem. 21: 1516-1521.

Tadros, W., A. L. Goldman, T. Babak, F. Menzies, L. Vardy, et al., 2007 SMAUG is a major regulator of maternal mRNA destabilization in *Drosophila* and its translation is activated by the PAN GU kinase. Dev. Cell 12: 143-155.

Wehr, K., A. Swan, and T. Schüpbach, 2006 Deadlock, a novel protein of *Drosophila*, is required for germline maintenance, fusome morphogenesis and axial patterning in oogenesis and associates with centrosomes in the early embryo. Dev. Biol. 294: 406-417.

Zaessinger, S., I. Busseau, and M. Simonelig, 2006. Oskar allows *nanos* mRNA translation in *Drosophila* embryos by preventing its deadenylation by Smaug/CCR4. Development 133: 4573-4583.

Figure Legends

Fig. 1. Dark-field photographs of cuticle preparations of RNAi knockdown embryos. Three embryos are illustrated from each knockdown line to capture the range of phenotypic severity that was observed. Embryos are oriented with anterior to the left. Control wild-type (wt) embryos are shown in the top row. The phenotypes observed for each line are discussed in Results.

Fig. 2. Embryos derived from RNAi knockdown mothers were stained for Vas protein (green) to visualize pole cells. Two embryos are shown for each knockdown line. For those that develop

sufficiently, the embryo in the left panel is at blastoderm stage, while the embryo in the right panel is at stage 10, the stage at which pole cells are in mid-migration, or later. In many cases development does not progress normally beyond the blastoderm stage, and in these instances the embryo in the right panel represents what appears to be the latest stage of development achieved. In some cases development ceases before cellularization, and then two representative embryos are shown. Wild-type embryos (wt), for comparison, are shown in the first row. The phenotypes observed for each line are discussed in Results.

Fig. 3. Embryos derived from RNAi knockdown mothers were stained for Vas protein (green) to visualize pole cell migration defects. Wild-type embryos, for comparison, are shown in the first picture. The phenotypes observed for each line are discussed in Results.

Fig. 4. Dark-field photographs of dorsal appendage defects of RNAi knockdown embryos. Two embryos are illustrated from each knockdown line to capture the range of phenotypic severity that was observed. Wild-type embryos (wt), for comparison, are shown in the first row. The phenotypes observed for each line are discussed in Results.

Fig. 5. Ovaries derived from RNAi knockdown mothers that did not lay eggs were visualized by DAPI staining (blue). Wild-type ovaries, for comparison, are shown in the first picture, and the oocyte (oo), 15 nurse cells (nc) and follicle cells (fc) are labelled. The phenotypes observed for each line are discussed in Results. In the bottom-right panel, a single wild-type ovariole and

two entire ovaries from the *Hip14* shRNA expressing line are photographed together to illustrate the difference in size and extent of development.

Fig. 6. Analysis of the efficacy of knockdown of each gene by RT-PCR analysis. The name of the targeted gene and 4 lanes of gel are shown in each small picture. In each picture, cDNA prepared from wild-type embryos were added in lanes 1-2 and cDNA prepared from RNAi knockdown embryos were added in lanes 3-4. Primers amplifying the indicated gene were used in lanes 1 and 3 to compare cDNA level in wild-type and knockdown lines. Primers amplifying a control gene knockdown and primers of rp49 were used in lanes 2 and 4. Knockdown is most efficient when the band in lane 3 is absent or very much weaker than the band in lane 1 while the bands in lanes 2 and 4 are equally intense. The percentage value in each panel reports the following ratio of band intensities: (lane 3/lane 1) / (lane 4/lane 2). This value measures the efficiency of the knockdown when controlled for potential differences in the amount of RNA used for the PCR reaction in the control and knockdown lanes. 0% represents a total knockdown and 100% represents a completely ineffective knockdown. Band intensities were quantitated using ImageJ software.

Fig. 7. *del* RNAi affects early pole plasm formation. Ovaries derived from RNAi knockdown mothers who lay eggs, but where pole cells do not form, were immunostained for Vas protein (green) and Osk protein (red) to visualize pole plasm formation. Nuclei were visualized by DAPI staining (blue). Wild-type ovaries, for comparison, are shown in the first row. ***del RNAi***:

Accumulation of VAS at the oocyte posterior and nuage in nurse cells is reduced while cytoplasmic nurse cell VAS levels are normal. Posterior OSK levels are also reduced.

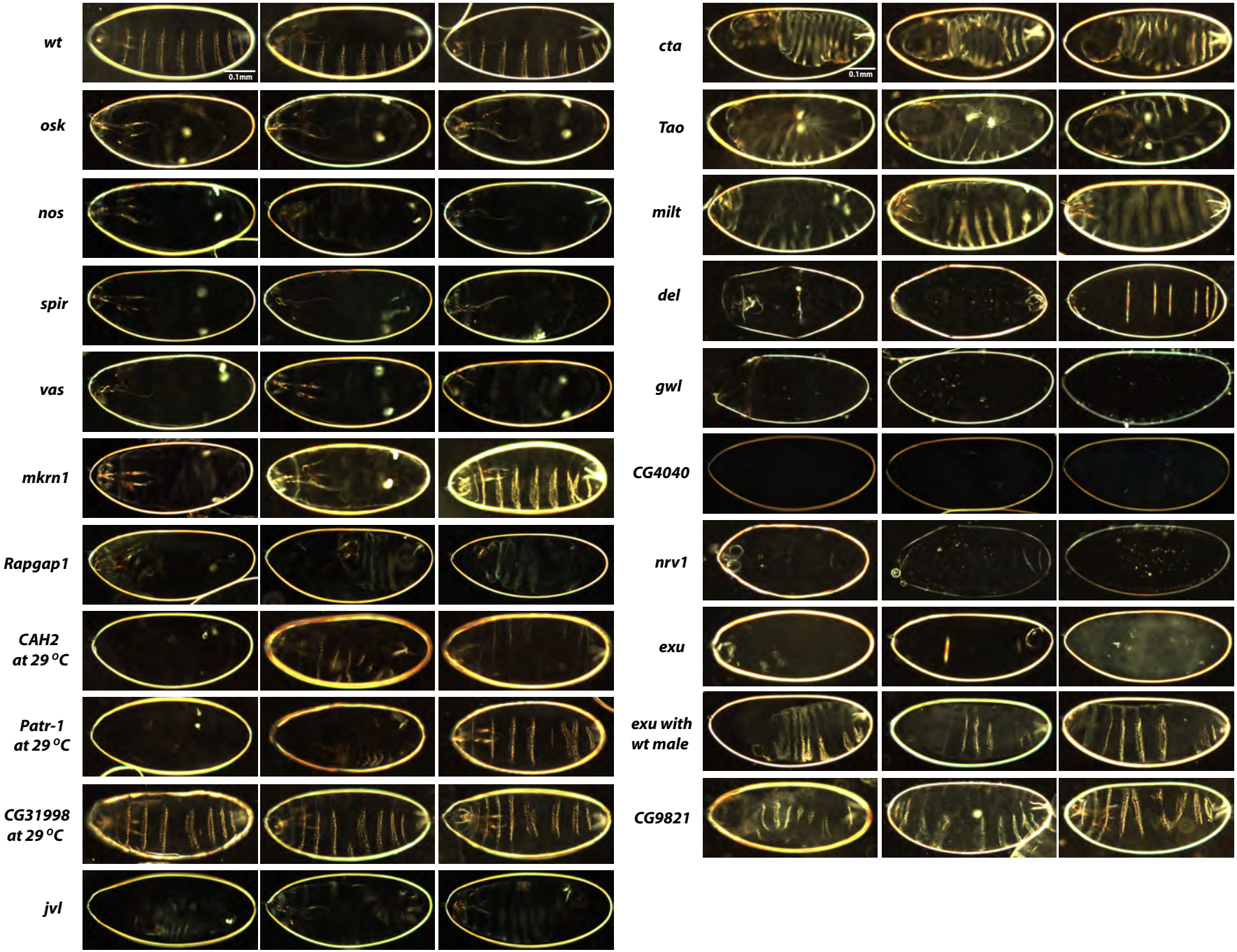

Liu and Lasko Figure 1

Fig. 2.

Pole cell staining

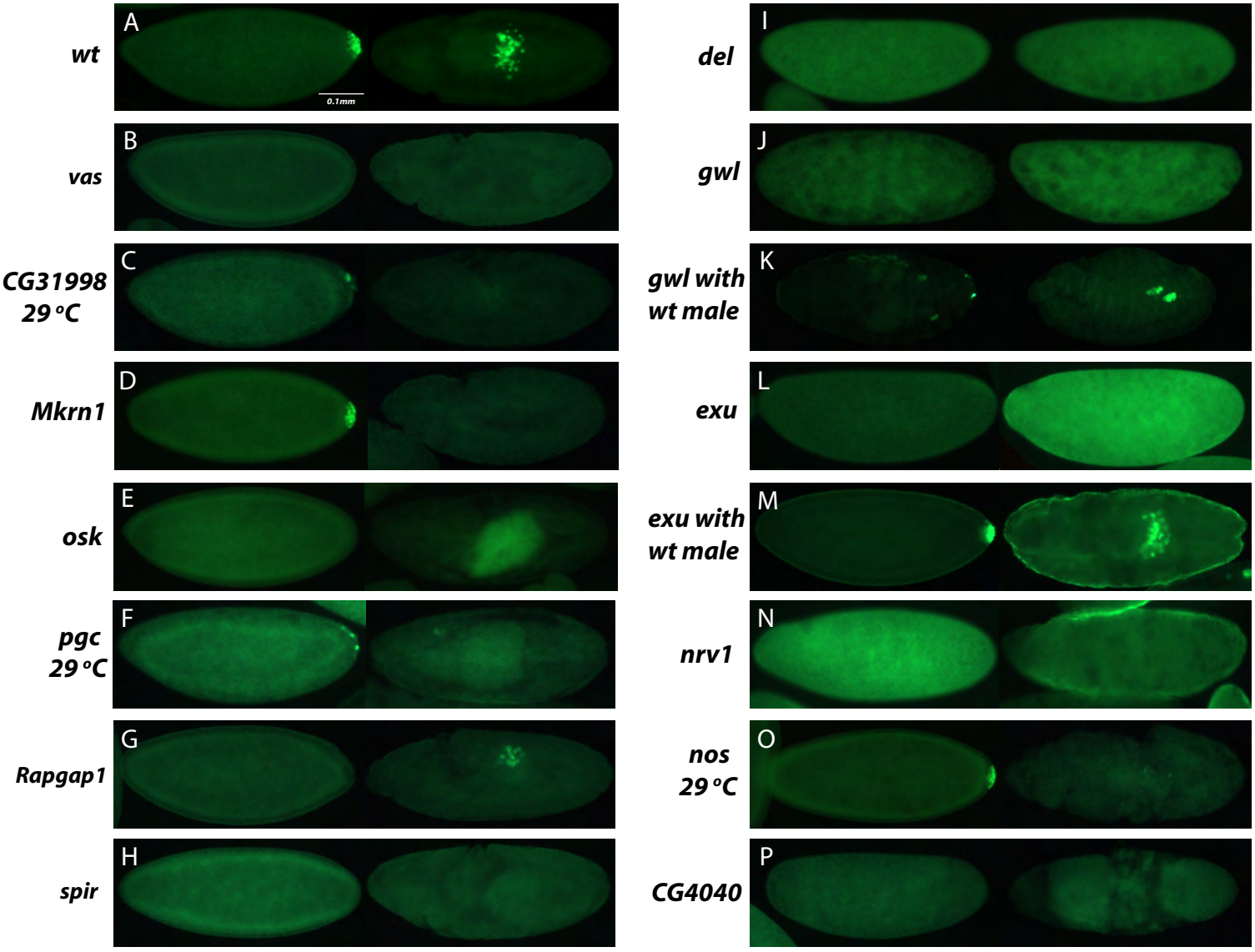

Fig. 3.

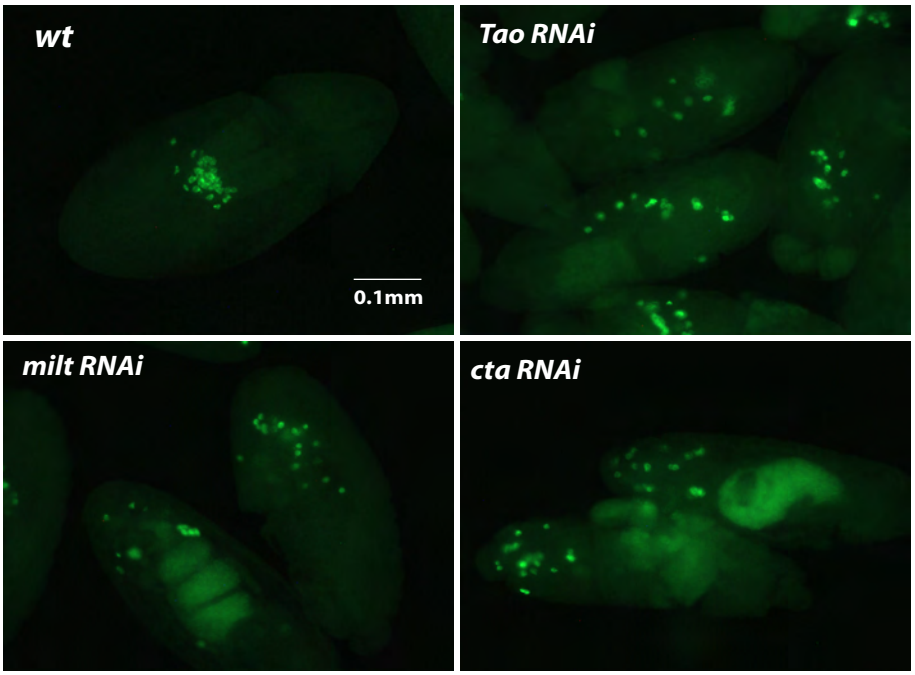

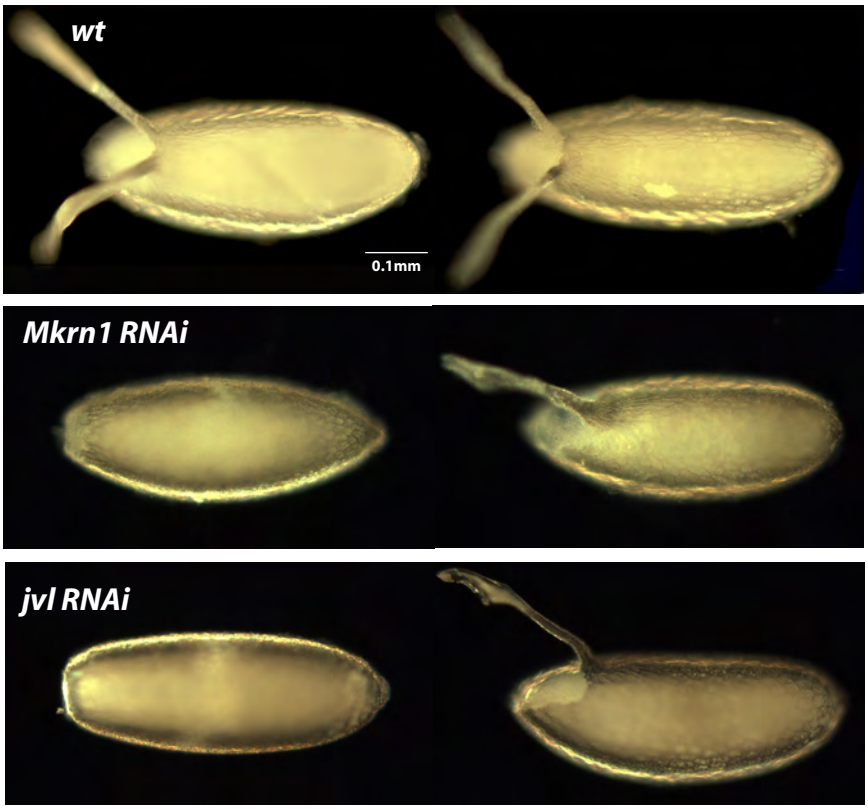

Liu and Lasko Figure 4

Fig. 5.

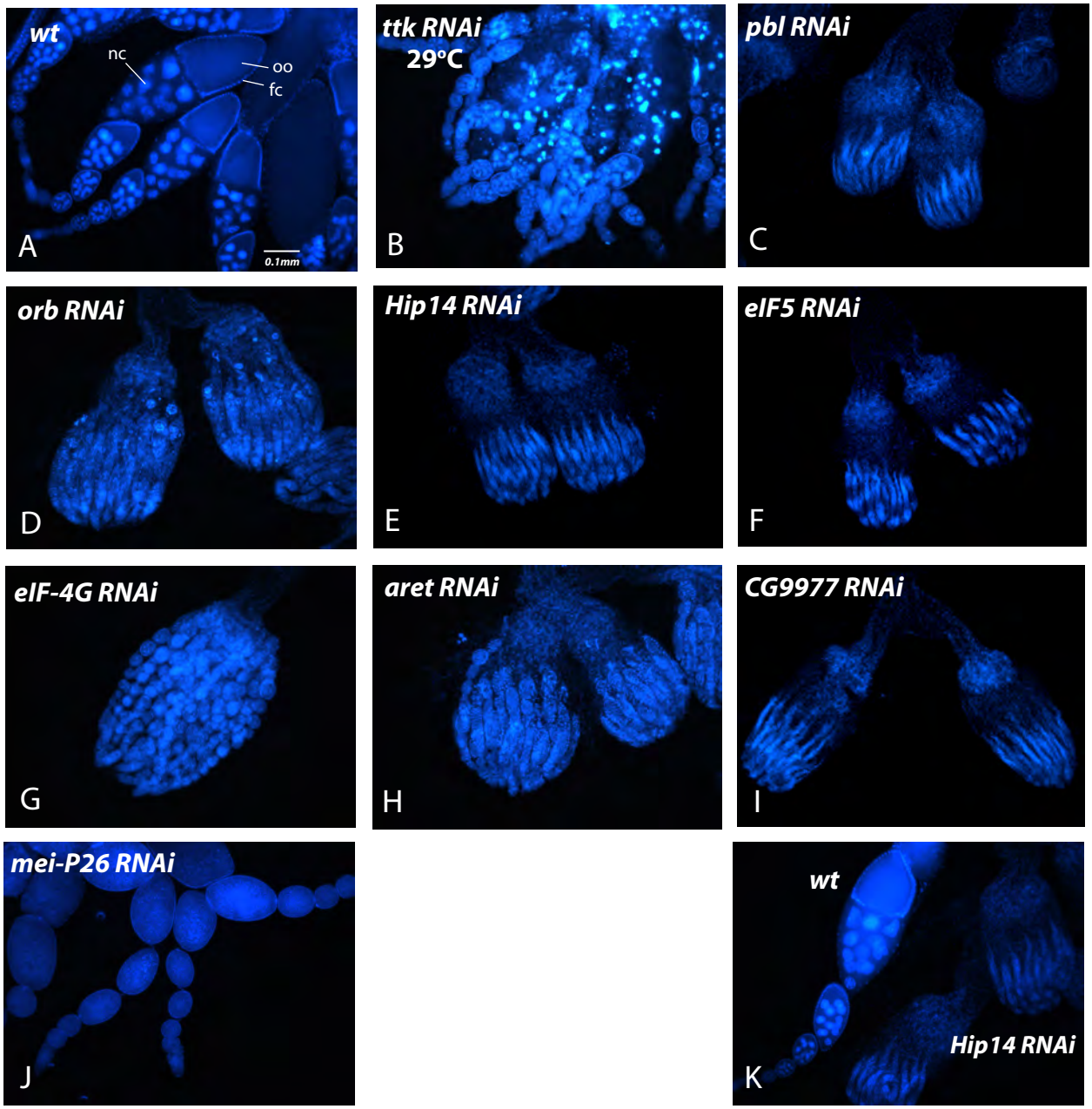
wt
nc
oo
fc
A
0.1mm
ttk RNAi
29°C
B
pbl RNAi
C
orb RNAi
D
Hip14 RNAi
E
eIF5 RNAi
F
eIF-4G RNAi
G
aret RNAi
H
CG9977 RNAi
I
mei-P26 RNAi
J
wt
Hip14 RNAi
K

Fig. 6.

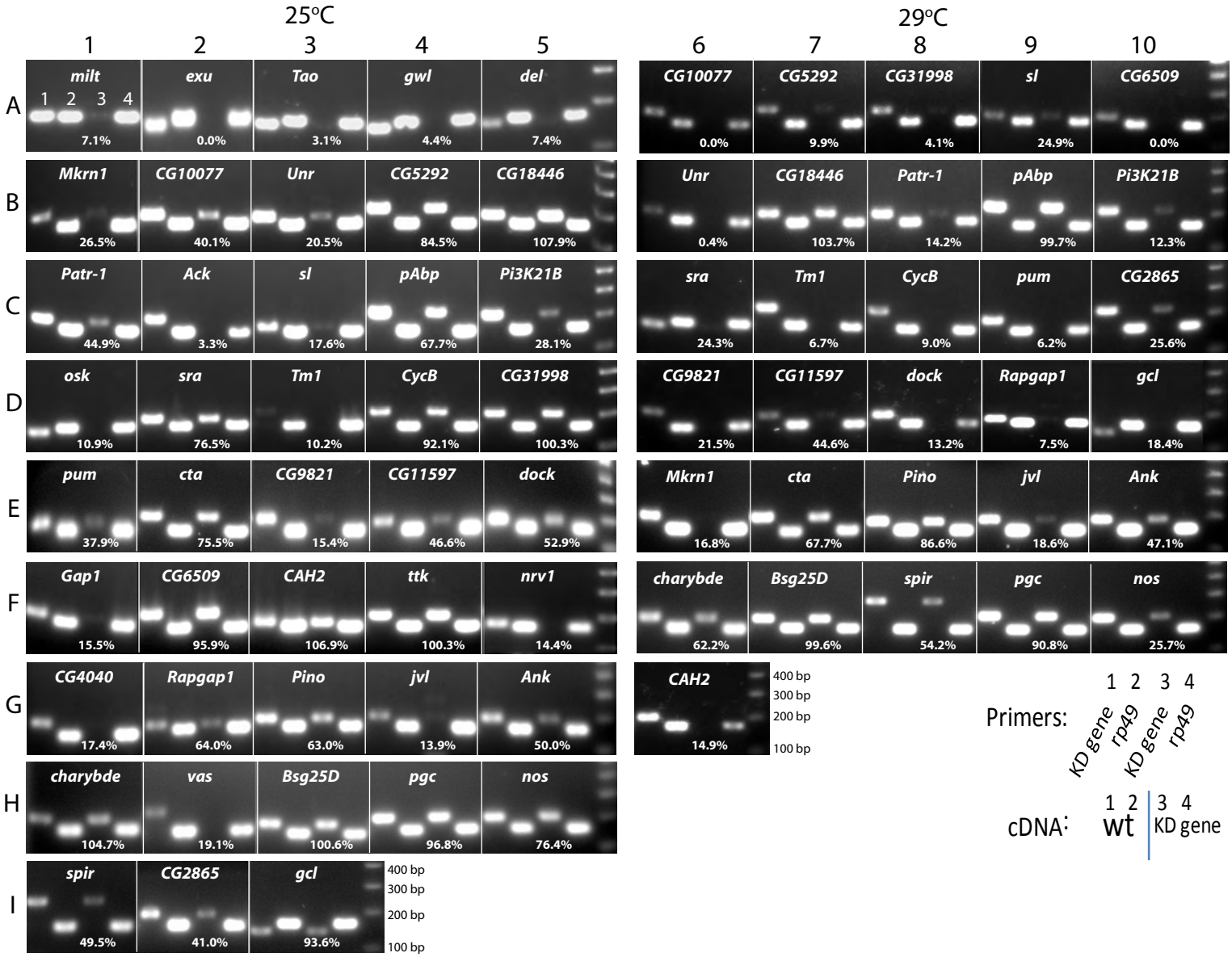
25°C
29°C
1 2 3 4 5
6 7 8 9 10
A
milt 1 2 3 4 7.1%
exu 0.0%
Tao 3.1%
gwl 4.4%
del 7.4%
CG10077 0.0%
CG5292 9.9%
CG31998 4.1%
sl 24.9%
CG6509 0.0%
B
Mkrn1 26.5%
CG10077 40.1%
Unr 20.5%
CG5292 84.5%
CG18446 107.9%
Unr 0.4%
CG18446 103.7%
Patr-1 14.2%
pAbp 99.7%
Pi3K21B 12.3%
C
Patr-1 44.9%
Ack 3.3%
sl 17.6%
pAbp 67.7%
Pi3K21B 28.1%
sra 24.3%
Tm1 6.7%
CycB 9.0%
pum 6.2%
CG2865 25.6%
D
osk 10.9%
sra 76.5%
Tm1 10.2%
CycB 92.1%
CG31998 100.3%
CG9821 21.5%
CG11597 44.6%
dock 13.2%
Rapgap1 7.5%
gcl 18.4%
E
pum 37.9%
cta 75.5%
CG9821 15.4%
CG11597 46.6%
dock 52.9%
Mkrn1 16.8%
cta 67.7%
Pino 86.6%
jvl 18.6%
Ank 47.1%
F
Gap1 15.5%
CG6509 95.9%
CAH2 106.9%
ttk 100.3%
nrv1 14.4%
charybde 62.2%
Bsg25D 99.6%
spir 54.2%
pgc 90.8%
nos 25.7%
G
CG4040 17.4%
Rapgap1 64.0%
Pino 63.0%
jvl 13.9%
Ank 50.0%
CAH2 14.9%
400 bp
300 bp
200 bp
100 bp
H
charybde 104.7%
vas 19.1%
Bsg25D 100.6%
pgc 96.8%
nos 76.4%
I
spir 49.5%
CG2865 41.0%
gcl 93.6%
400 bp
300 bp
200 bp
100 bp
Primers:
1 2 3 4
KD gene
rp49
KD gene
rp49
cDNA:
1 2
wt
3 4
KD gene

Fig. 7.

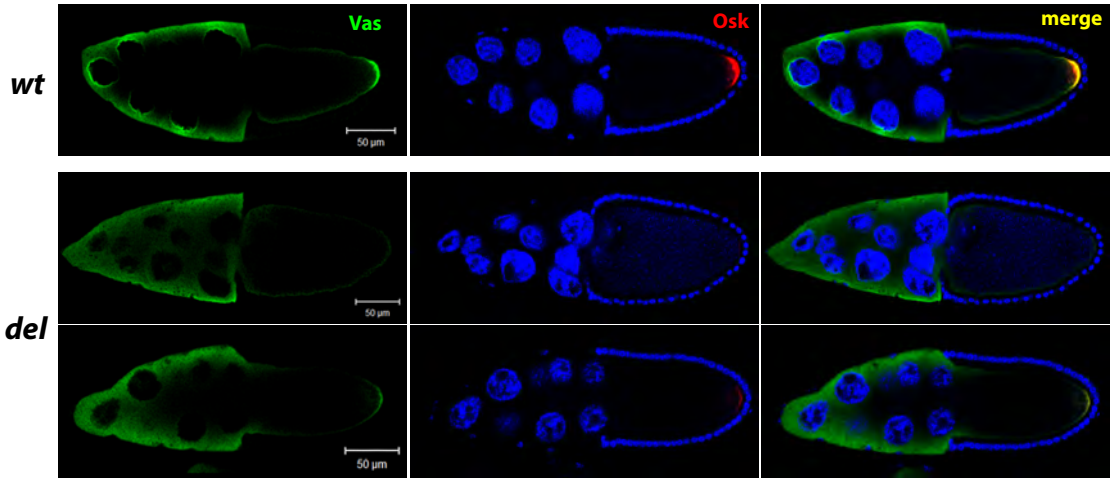

Table 1. Summary of visible phenotypes of RNAi knockdown mothers. * RNAi stock not available.

Gene name	Hatch rate at 25°C	Hatch rate at 29°C	Egg laying	Cuticle defect	Pole Cell formation defect	Pole cell migration defect	Dorsal appendage defect	Bloomington stock number	TRiP number
wt	93%	84%	yes	--	--	--	--		
Ack	>80%		yes	--	--	--	--	35264	GL00158
Ank	>80%	67%	yes	--	--	--	--	43965	GL01575
aret			no					35394	GL00314
Bsg25D	>80%	>80%	yes	--	--	--	--	36828	GL01064
CAH2	>80%	62%	yes	+	--	--	--	41836	GL01264
CG10077	>80%	73%	yes	--	--	--	--	32388	HMS00380
CG11597	>80%	>80%	yes	--	--	--	--	43175	GL01517
*CG14322**								N/A	
CG18446	>80%	78%	yes	--	--	--	--	33735	HMS00618
CG2865	>80%	71%	yes	--	--	--	--	43165	GL01507
CG31998	>80%	12%	yes	++	++	--	--	41828	GL01256
*CG3295**								N/A	
CG4040	0%		yes	+++	+++		--	42776	GL01145
CG5292	>80%	>80%	yes	--	--	--	--	32499	HMS00502
CG6509	>80%	78%	yes	--	--	--	--	41832	GL01260
CG9821	68%	55%	yes	++	--	--	--	43171	GL01513
CG9977			no					43168	GL01510
charybde	>80%	>80%	yes	--	--	--	--	43975	GL01585
cta	5%	0%	yes	+++	--	+++	--	41964	HMS02361
CycB	>80%	>80%	yes	--	--	--	--	39024	HMS01943
del	0%		yes	+++	+++		--	32375	HMS00366
dock	>80%	77%	yes	--	--	--	--	43176	GL01519
eIF-4G			no					33049	HMS00762
eIF5			no					34841	HMS00159
exu	0%		yes	+++	+++		--	41816	GL01244
Gap1	>80%		yes	--	--	--	--	41830	GL01258
gcl	>80%	>80%	yes	--	--	--	--	34608	HMS00602
gwl	0%		yes	+++	+++		--	35212	GL00091
Hip14			no					35012	HMS01422
jvl	78%	36%	yes	++	--	--	++	43177	GL01520
mei-P26			no					36855	GL01124
milt	41%		yes	++	--	++	--	43173	GL01515
Mkrn1	76%	78%	yes	++	++	--	++	43178	GL01521
nos	1.5%	0%	yes	+++	++		--	33973	HMS00930
nrv1	0%		yes	+++	+++		--	41829	GL01257
orb			no					43143	GL01484
osk	0%		yes	+++	+++		+++	36903	GL01101
pAbp	>80%	69%	yes	--	--	--	--	36127	HMS01542
Patr-1	>80%	47%	yes	+	--	--	--	34667	HMS01144
pbl			no					36841	GL01092
pgc	>80%	>80%	yes	--	+	--	--	33720	HMS00601
Pino	>80%	>80%	yes	--	--	--	--	43971	GL01581
Pi3K21B	>80%	59%	yes	--	--	--	--	36810	GL01028
pum	>80%	>80%	yes	--	--	--	--	41875	GL01307
Rapgap1	72%	48%	yes	++	++	--	--	42782	GL01152
sl	>80%	78%	yes	--	--	--	--	35604	GL00444
spir	21%	8%	yes	+++	+++		--	43161	GL01503
sra	>80%	66%	yes	--	--	--	--	36900	GL01096
Tao	0%		yes	+++	--	++	--	35147	GL00015
Tm1	>80%	>80%	yes	--	--	--	--	38232	HMS01676
ttk	>80%		no (29°C)					36748	HMS03008
Unr	>80%	>80%	yes	--	--	--	--	32432	HMS00428
vas	0%		yes	+++	+++		--	38924	GL01013